The hepatotoxic fluoroquinolone trovafloxacin disturbs TNF- and LPS-induced p65 nuclear translocation in vivo and in vitro

Giustarini, G.; Huppelschoten, S.; Barra, M.; Oppelt, A.; Wagenaar, L.; Weaver, R.J.; ... ; Pieters, R.H.H.

Toxicology and Applied Pharmacology 391 (2020) 114915

Contents lists available at ScienceDirect

Toxicology and Applied Pharmacology

journal homepage: www.elsevier.com/locate/taap

The hepatotoxic fluoroquinolone trovafloxacin disturbs TNF- and LPS-induced p65 nuclear translocation in vivo and in vitro

Giulio Giustarini[a,*], Suzanna Huppelschoten[b], Marco Barra[a,e], Angela Oppelt[c], Laura Wagenaar[a], Richard J. Weaver[d], Marianne Bol-Schoenmakers[a], Joost J. Smit[a], Bob van de Water[b], Ursula Klingmüller[c], Raymond H.H. Pieters[a]

[a] Immunotoxicology, Institute for Risk Assessment Sciences, Faculty of Veterinary Medicine, Utrecht University, Utrecht, the Netherlands
[b] Division of Drug Discovery and Safety, Leiden Academic Centre for Drug Research, Leiden University, Leiden, the Netherlands
[c] Division Systems Biology of Signal Transduction, German Cancer Research Center (DKFZ), Heidelberg, Germany
[d] Biopharmacy, Institut de Recherches Internationales Servier (I.R.I.S.), Suresnes 92284, France
[e] University of Pisa, Department of Pharmacy, Italy

ARTICLE INFO

Keywords:
Drug-induced liver injury
Trovafloxacin
Inflammation
NF-κB
TNF
LPS

ABSTRACT

Idiosyncratic drug-induced liver injury (IDILI) is a severe disease that cannot be detected during drug development. It has been shown that hepatotoxicity of some compounds associated with IDILI becomes apparent when these are combined in vivo and in vitro with LPS or TNF. Among these compounds trovafloxacin (TVX) induced apoptosis in the liver and increased pro-inflammatory cytokines in mice exposed to LPS/TNF. The hepatocyte survival and the cytokine release after TNF/LPS stimulation relies on a pulsatile activation of NF-κB.

We set out to evaluate the dynamic activation of NF-κB in response to TVX + TNF or LPS models, both in mouse and human cells. Remarkably, TVX prolonged the first translocation of NF-κB induced by TNF both in vivo and in vitro. The prolonged p65 translocation caused by TVX was associated with an increased phosphorylation of IKK and MAPKs and accumulation of inhibitors of NF-κB such as IκBα and A20 in HepG2. Coherently, TVX suppressed further TNF-induced NF-κB translocations in HepG2 leading to decreased transcription of ICAM-1 and inhibitors of apoptosis. TVX prolonged LPS-induced NF-κB translocation in RAW264.7 macrophages increasing the secretion of TNF. In summary, this study presents new, relevant insights into the mechanism of TVX-induced liver injury underlining the resemblance between mouse and human models. In this study we convincingly show that regularly used toxicity models provide a coherent view of relevant pathways for IDILI. We propose that assessment of the kinetics of activation of NF-κB and MAPKs is an appropriate tool for the identification of hepatotoxic compounds during drug development.

1. Introduction

Drug-induced liver injury (DILI) is a complex disease of concern to pharmaceutical companies and health care providers (Chalasani et al., 2015; Fontana et al., 2009). The identification of mechanisms behind most idiosyncratic DILI (IDILI) remains a challenge that needs to be solved in order to improve drug safety (Weaver et al., 2017). A prevalent hypothesis to explain the aetiology and patient specific response to certain drugs is represented by the "inflammatory hypothesis" (Roth et al., 2017) proposing that the liver-toxic potential of a number of pharmaceuticals results from a combination of sterile and non-sterile inflammatory stimuli (Buchweitz, 2002; Deng et al., 2006; Dugan and MacDonald, 2010; Lu et al., 2012; Luyendyk, 2003; Zou et al., 2009). The initial insult caused by the combination of drug and inflammatory stimuli as described in this hypothesis is embedded in the so-called "the danger hypothesis" (Matzinger and Kamala, 2011). The latter may explain how cellular damage triggers hypersensitivity-like hepatic adverse drug reaction (Pirmohamed et al., 2002).

In the last decade, many studies have underlined the importance of cellular damage and innate immunity in the development of drug-induced liver toxicity (Fredriksson et al., 2011; Shaw et al., 2009b; Beggs et al., 2014; Giustarini et al., 2018; Fredriksson et al., 2014; Herpers et al., 2016). In particular, tumor necrosis factor (TNF) appears to be involved in the liver toxicity of some DILI-associated compounds but the interactions between TNF signaling and these pharmaceuticals remain to be further elucidated.

* Corresponding author at: Yalelaan 104, 3584CM Utrecht, the Netherlands.
E-mail addresses: g.giustarini@uu.nl (G. Giustarini), r.h.h.pieters@uu.nl (R.H.H. Pieters).

https://doi.org/10.1016/j.taap.2020.114915
Received 20 October 2019; Received in revised form 10 January 2020; Accepted 5 February 2020
Available online 06 February 2020
0041-008X/

Among these DILI-associated compounds the fluoroquinolone trovafloxacin (TVX) is well studied and it is shown that TVX, when administered in combination with lipopolysaccharide (LPS) or TNF to mice induces severe liver toxicity associated with vast apoptotic areas in the liver, increased serum levels of alanine amino transferases (ALT) and pro-inflammatory cytokines (Shaw et al., 2009b, 2009a; Giustarini et al., 2018). TNF exerts many biological effects that are mediated by engagement of TNF-receptor 1 (TNF-R1) and TNF-receptor 2 (TNF-R2). The most important difference between the two receptors for TNF is that the cytoplasmic tail of TNF-R1 contains a protein-protein interaction domain called "death domain" whereas TNF-R2 does not. The death domain interacting with TNF-R1-associated death domain can form two different complexes of signaling proteins called complex I and II (Wullaert et al., 2006). TNF-induced pro-survival signaling occurs via complex I, which mediates activation of NF-κB and MAPK, whereas death signaling via complex II activates caspase 8 (Wullaert et al., 2006). In particular, nuclear translocation of NF-κB (consequent of pathway activation) mediates usually pro-survival effects, especially in hepatocytes regulating activation of JNK. Indeed, inhibition of TNF-induced NF-κB nuclear translocation is associated with sensitization of hepatocytes to cell death via sustained JNK activation which terminates with caspase activation (Liu et al., 2002).

Several other studies have pointed to the importance of NF-κB in the survival of hepatocytes as well as in the synthesis of inflammatory cytokines upon TNF stimulation (Wullaert et al., 2007; Sakai et al., 2017). NF-κB has a similar function in macrophages when exposed to LPS, since Toll-like receptor signaling in liver-resident macrophages increased translocation of NF-κB into the nucleus and consequently transcription of various cytokines (Sakai et al., 2017).

In this study, we wanted to examine whether TVX causes alterations of NF-κB pathway activated by TNF or LPS. Here, we found that TVX perturbs NF-κB-mediated transcription leading to accumulation of inhibitors of NF-κB pathway via a prolonged activation of IKKα/β. This together with the simultaneously prolonged activation and reactivation of MAPKs may explain the observed increase in cytokine production and induction of apoptosis as result of TVX treatment.

2. Materials and methods

2.1. Animals and experimental set up

Male, 9 to 11-week old, C57BL/6 J mice (The Jackson Laboratory, Charles River) were used for all experiments. They were allowed to acclimate for 1 week in a 12 h light/dark cycle,mean temperature of 23 ± 2 °C and 50–55% relative humidity. Acidified drinking water and laboratory food pellets were provided ad libitum.

Mice were fasted 7 h prior to treatment. TVX (150 mg/kg), levofloxacin (LVX, 375 mg/kg), or saline vehicle (Veh) was administered orally 3 h before recombinant murine TNF injection (50 μg/kg, i.p.) (Shaw et al., 2009b). Food was available again immediately after TNF administration. Animals analyzed at time point 0 h did not receive TNF (Fig. 1).

In vivo studies were approved by the Ethics Committee for Animal Experiments of Utrecht University and complied with governmental and international guidelines on animal experimentation.

2.2. Chemicals

TVX, LVX and LPS were purchased from Sigma-Aldrich (St. Louis, MO, USA). Recombinant murine TNF was purchased from R&DSystems (Minneapolis, MN, USA).

2.3. Cell culture

HepG2 human hepatoblastoma cells and RAW264.7 murine monocyte/macrophage cells (American Type Culture Collection, Manassas, VA, USA) were maintained in MEM + Glutamax (Gibco, Invitrogen, Carlsbad, CA, USA) supplemented with 10% fetal bovine serum (FBS) in 75 cm^2 tissue culture treated flasks. Cells were cultured in a humidified atmosphere composed of 95% air and 5% CO2 and a temperature of 37 °C. HepG2 cells were passaged twice each week. 0.25% Trypsin-EDTA was used to detach confluent HepG2 cells from the flask. After plating, cells were allowed to adhere 48 h before treatment.

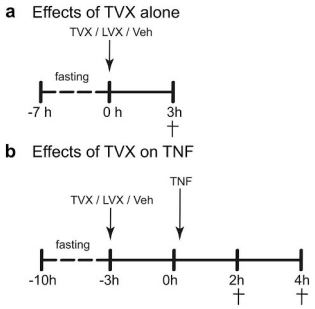

Fig. 1. Protocol for the treatment of mice in the TVX + TNF model of drug-induced liver injury.
Mice were fasted for 7 h and then administered with an intragastric gavage of the drug solutions or saline (Veh). Three hours later, mice were either killed to observe the effects of the drugs alone (a) or received an intraperitoneal injection of TNF (b). TNF-injected mice were subsequently killed after 2 and 4 h. Two hours after TNF was the selected time point to assess the effects of drugs on TNF-induced transcription and p65 nuclear translocation. Livers of mice culled at 4 h were used to confirm the occurrence of the damage. LVX, levofloxacin; TNF, tumor necrosis factor; TVX, trovafloxacin; Veh, vehicle.

TVX and LVX was reconstituted to a stock solution of 200 mM in dimethyl sulfoxide (DMSO) and diluted in culture medium to the desired concentrations. The final DMSO concentrations did not exceed 0.025% (V/V). Recombinant human TNF was reconstituted to a stock solution of 100 mg/mL in PBS + 0.3% BSA as indicated by the manufacturer (R&DSystems). After incubation with the fluoroquinolones with or without TNF, HepG2 cells were washed with PBS, after treated with cytoplasmic lysis buffer (10 mM Hepes; pH 7.9, 10 mM KCl, 0.1 mM EDTA, 0.1 mM EGTA, 0.4% NP-40, protease and phosphatase inhibitors) and gently scraped. The suspensions were collected and left on ice for 20 min before centrifugation 13,000 rpm for exactly 1 min at 4 °C. Supernatant was collected and immediately stored at -80 °C. The pellets were washed 3 times with cytoplasmic lysis buffer without NP-40. Nuclei were resuspended and sonicated in nuclear lysis buffer (20 mM Hepes pH 7.9, 25% glycerin, 400 mM NaCl, 1 mM EDTA, 1 mM EGTA, 0.8% NP-40, protease and phosphatase inhibitors). Suspension were centrifuged at 13000 rpm for 5 min at 4 °C. Supernatant was collected and immediately stored at -80 °C.

HepG2 RelA-GFP (NF-κB, p65), A20-GFP BAC and ICAM-1 BAC GFP reporter cell lines were previously established and characterized (Wink et al., 2017, 2018). HepG2 BAC GFP reporters were maintained and exposed to drugs in DMEM high glucose supplemented with 10% (V/V) FBS, 25 U/mL penicillin and 25 μg/mL streptomycin. The cell lines were used between passage 5 and 25. For live cell imaging, the cells were seeded in Greiner black μ-clear 96 wells plates, at 50000 cells per well. After plating, cells were allowed to adhere 48 h before treatment.

RAW264.7 cells were passaged twice each week and a scraper was used to detach them from the flask. LPS was reconstituted to a stock solution of 1 mg/mL in PBS as indicated by manufacturer. After plating 15×10^4 cells in each of the 12 wells, cells were allowed to adhere 48 h before treatment. Drug treatment was similar as with HepG2 cells. RAW264.7 cells were either exposed to the drugs alone for 4 h or for 2 h before receiving LPS (10 ng/mL). Cells for imaging were seeded in IBIDI μ-slide 8 well, washed once with PBS and fixed with 4% formaldehyde, permeabilized with 0.2% triton X-100 in PBS, and blocked with 1.5% normal donkey serum. Polyclonal antibodies against anti-NF-κB p65 (1 μg/well) were applied for 1 h followed by an 1 h incubation with

FITC-conjugated donkey anti-rabbit IgG. The presence of cell nucleus was determined with DAPI. After washing with PBS, the coverslips were mounted in SlowFade Diamond (Thermo scientific, Rockford, IL, USA).

2.4. Cell death analysis

Induction of apoptosis in real time was quantified using a live cell apoptosis assay previously described (Puigvert et al., 2010). Briefly, binding of annexin V-Alexa633 conjugate to phosphatidyl serine on the membranes of apoptotic cells, intracellular fluorescence of propidium iodide (PI) in cells stained with Hoechst (nuclear staining) was followed in time by a Nikon TiE2000 confocal laser microscope.

Overall cell death (loss of membrane integrity) was determined by lactate dehydrogenase (LDH) release in the medium in essentially the same manner as described (Van de Water et al., 2001).

2.5. Microscopy

Accumulation of GFP levels, PI and Hoechst staining was monitored using a Nikon TiE2000 confocal laser microscope (lasers 540, 488 and 408 nm), equipped with an automated stage and perfect focus system at 37 °C with humidified atmosphere and 5% CO_2/air mixture. All imaging was similar as previously described. 96-well plate contained one reporter cell line, which was exposed to all the compounds used (TVX, LVX or DMSO). For the ICAM1-GFP reporter experiments, cells were first exposed for 8 h to compound only; next, TNFα was added to all wells, up to a final concentration of 4 ng/mL. Directly after TNFα treatment the live cell imaging was started.

HepG2 RelA-GFP (NF-κB, p65) and A20-GFP BAC reporter cell lines were generated and characterized as described previously (Wink et al., 2017; Herpers et al., 2016). Accumulation of GFP levels or nuclear translocation, and Hoechst staining was monitored using a Nikon TiE2000 confocal laser microscope (lasers: 640, 540, 488, and 408 nm). This microscope is equipped with an automated stage and perfect focus system at 37 °C with humidified atmosphere and 5% CO2/air mixture. HepG2 cells were stained with 50 ng/mL Hoechst33342 for 30 min to visualize the nuclei. The Hoechst medium was replaced with exposure medium containing the drugs and a final concentration of 4 ng/mL TNF. To prevent a delay in TNF response in the oscillations of the RelA-GFP reporter, solutions were added at the microscope per well, directly upon imaging of the first image (t = 0).

Half of the biggest liver lobe was embedded in optimal cutting temperature compound (OCT) and 8 μm liver slices were prepared for immunohistochemistry. Slices were fixed with acetone and permeabilized with 0.2% triton X-100 in PBS, and blocked with 1.5% normal donkey serum. Polyclonal antibodies against anti-NF-κB p65 (10 μg/slide) were applied for 1 h followed by an 1 h incubation with FITC-conjugated donkey anti-rabbit IgG. The presence of cell nucleus was determined with DAPI. After washing with PBS, the coverslips were mounted in SlowFade Diamond (Thermo scientific, Rockford, IL, USA). Three liver slices per treatment derived from three different animals were stained and assessed on the same slide. Hepatocyte nuclei were selected based on the intensity and area of DAPI. Nuclear count was stopped to the lowest number of nuclei counted in one of the group of treatment. For RAW264.7 cells and liver slices images were acquired with Olympus BX-60 microscope equipped with Leica CCD camera (Leica DFC425C) (40 × 0.5 objective).

2.6. Image analysis of fluorescent protein reporter activity

Quantitative image analysis was performed with CellProfiler version 2.1.1 (Kamentsky et al. 2011) with an in house developed CellProfiler module implementing the watershed masked algorithm for segmentation (Yan and Verbeek 2012; Wink et al., 2017). Image analyses results were stored as HDF5 files. Data analysis, quality control and graphics were performed using the in house developed R package h5CellProfiler. For each reporter intensity levels of the GFP signal, the nuclear Hoechst33342 intensity levels and at 24 h the PI staining were measured at the single cell level.

2.7. Western blot analyses

Approximately 50 mg of each liver sample was lysed using 500 μL RIPA lysis buffer (Thermo scientific, Rockford, IL, USA) containing protease and phosphatase inhibitors (Roche Applied Science, Penzberg, Germany). The total protein concentration of liver lysates and nuclear and cytoplasmic fractions of cell lines were measured by the BCA protein assay kit (Thermo scientific, Rockford, IL, USA). Standardized protein amounts (30 μg) of boiled samples were analyzed by electrophoresis in SDS-PAGE gel 4–20% or 7.5% and electro-transferred onto polyvinylidene difluoride membranes (Bio-Rad, Veenendaal, The Netherlands). Membranes were blocked with immersion in ethanol 100% for 1 min and afterwards rehydrated with TBS supplemented with 0.2% Tween (TBS-T) and incubated overnight with: anti-human p65 (Abcam, ab16502); anti-human phospho-p65 (Ser536) (Cell signaling Rabbit #3031S); anti-human clathrin HC (Cell signaling, #2410), anti-human lamin A/C (Cell signaling #2032); anti-human IκBα (Cell Signaling, #9242), anti-human phospho-p44/42 (Erk1/2) (Thr202/Tyr204) (Cell Signaling, #9101); anti-human phospho-p38 (Thr180/Tyr182) (Cell Signaling, #9211); anti-human phospho-IκBα (Ser32, clone: 14D4) (Cell signaling, #2859), anti-human phospho-IKKα/β (Ser176/180, clone; 16A6), (Cell signaling, #2697), anti-human phospho-SAPK/JNK (Thr183/Tyr185, clone: 81E11) (Cell Signaling, #4668). After washing in TBS-T, the membranes were incubated with rabbit anti-goat peroxidase-conjugated secondary antibody (1:5000, Dako, Glostrup, Denmark) for 1 h at room temperature. Finally, membranes were washed in TBS-T and once in TBS, incubated with ECL Prime Western Blotting Detection Reagent (Amersham Biosciences, Roosendaal, The Netherlands), and digital images were obtained with the ChemiDoc XRS Quantity One (Bio-Rad Laboratories, Hercules, CA, USA). In the next step the membranes were re-probed with a β-Actin or Lamin A/C antibody (1:4000, Cell Signaling, MA, USA) to assess the equality of loading. Signal intensities were quantified using ChemiDoc XRS Quantity One (Bio-Rad Laboratories, Hercules, CA, USA), and protein expression normalized with β-Actin.

2.8. qPCR

For mRNA studies, the medial part of the biggest liver lobe from each mouse (approximately 50 mg) was snap frozen in liquid nitrogen and stored at −80 °C untill RNA isolation. Each sample was suspended in 500 μL RNA InstaPure (Eurogentec) and homogenized using a TissueLyser (Qiagen, Hilden, Germany) for 1 min/25 Hz twice. The homogenized tissue was centrifuged for 10 min at 12,000 ×g. The supernatant, containing RNA in RNA Insta-Pure was transferred to a new vial and RNA was isolated using phenol-chloroform extraction. The amount of RNA was determined using the NanoDrop 2000 Spectrophotometer (ThermoScientific). Subsequently, 1 μg of extracted total RNA was reverse transcribed with the iScriptTM cDNA Synthesis kit (Bio-Rad Laboratories, Hercules, CA, USA). Quantitative reverse transcriptase PCR was performed suing a iCycler iQ system (Biorad), and amplification was done using iQ SYBR Green supermix (Biorad) with 0.3 μM final primer concentration. Primer sequences: mouse ICAM-1 FW-GCTACCATCACCGTGTATTCG and RV-TAGCCAGCACCGTGAATGTG, mouse A20 FW-GAACCAGATTCCATGAAGCAA and RV-CCTGTAGTTCGAGGCATGTC; mouse IκBα FW-AGGAGTACGAGCAAATGGTG and RV-CGGCTTCTCTTCGTGGATG; mouse c-IAP1 FW-TTGAGCAGCTGTTGTCCACTTC and RV-GGCCAAAATGCACCACTGT; mouse c-IAP2 FW-AGGGACCATCAAGGGCACAGTG and RV-TTGGCGGTGTCTCGTGCTATC; mouse MIP-2 FW- AAAGTTTGCCTTGACCCTGAAG and RV-CAGTTAGCCTTGCCTTTGTTCAGT; mouse TNF FW-AACGGCATGGATCTCAAAGA and RV-TTTCTCCTGGTATGAGATAGCAAATC, human

A20 FW-GCGTTCAGGACACAGACTTG and RV-TTCATCATTCCAGTTC CGAGTATC; human IκBα FW-GCTGAAGAAGGAGCGGCTACT and RV-TCGTACTCCTCGTCTTTCATGGA; human: IL-8 FW-CTCTTGGCAGCCT TCCTGATT and RV-TATGCACTGACATCTAAGTTCTTTAGCA; human c-IAP1 FW-AGCTGTTGTCAACTTCAGATACCACT and RV-TGTTTCACCA GGTCTCTATTAAAGCC; human c-IAP2 FW-ACTTGAACAGCTGCTATC CACATC and RV-GTTGCTAGGATTTTTCTCTGAACTGTC.

Gene specific primers were derived from the NCBI GenBank and were manufactured commercially (Eurogentec, Seraing, Belgium). For each sample, mRNA expression was normalized for the detected Ct value of GAPDH or β-actin. β-actin and GAPDH mRNA expressions were both tested showing no significant variations/in between differences in time and treatments. Data are expressed as fold increase compared with the control group (vehicle only).

2.9. Statistical analyses

Data are presented as means ± standard error of the mean (SEM). Statistical significance for comparisons was determined by ONE- or TWO-way ANOVA with Dunnett's post-hoc test. A P value less than 0.05 was considered statistically significant. All data are analyzed using GraphPad Prism (version 6.07) software (San Diego, CA, USA).

3. Results

3.1. Co-incubation with Trovafloxacin (TVX) and Tumor Necrosis Factor (TNF) induces apoptosis in HepG2 cells

HepG2 cells were exposed to TVX (20 μM), LVX (50 μM) or DMSO (0.01% max) for 24 h either in presence or in absence of TNF (4 ng/mL). TNF concentration used resembles that found in human blood during inflammatory stress (Copeland et al., 2005; Taudorf et al., 2007). Incubation of cells with TVX + TNF, but not with any of the other treatments, showed a gradual increase of Annexin V-staining and an increased leakage of LDH at 24 h. (Fig. 2a-b).

3.2. TVX disrupts TNF-induced p65 nuclear translocation

Because of the fundamental role of NF-κB in hepatocyte survival after TNF stimulation (Fredriksson et al., 2011) we decided to investigate the effects of TVX and LVX on TNF-induced NF-κB nuclear translocation in the liver of mice and in HepG2 cells. TNF was administered to the mice 3 h after single oral administration of drugs or vehicle (Fig. 1) and 2 h after the cytokine injection liver tissues were collected for immunofluorescence detection of nuclear and cytoplasmic p65 levels. TVX + TNF-treated mice showed a greater number of cells with increased nuclear/cytoplasmic p65 ratio in liver tissue when compared with LVX + TNF- or Veh + TNF-treated mice (Fig. 3a-b). Of note, liver tissue of these latter two groups did not show any significant difference in the distribution of p65 nuclear/cytoplasmic ratio values, but all treatments that included TNF significantly increased the number of hepatocytes with a high nuclear/cytoplasmic ratio when compared with Veh + PBS (Fig. 3a-b).

HepG2 cells have been shown to reproduce the TVX-induced transcriptional signature as observed in primary human hepatocytes (Liguori et al., 2008), indicating that HepG2 are good model cells to study TVX toxicity. To verify and describe in more detail the effect of TVX on the dynamics of p65 translocation we analyzed the kinetics of nuclear translocation of p65 using genetically modified p65-GFP-tagged HepG2 cells. All TNF treatments promoted a clear nuclear translocation of p65, and both LVX- and DMSO-treated cells displayed pulsatile oscillations of the p65 nuclear/cytoplasmic ratio after the exposure to TNF. TVX-treated cells showed a unique and sustained peak of p65 nuclear translocation occurring between 15 and 90 min after treatment, without further oscillations (Fig. 3c).

We confirmed the TVX-induced alterations of p65 translocation in non-mutant HepG2 using quantification of p65 protein levels in nuclear and cytoplasmic extracts of cells treated with DMSO + TNF or TVX + TNF and analyzed by Western blot (Fig. 3d). Simultaneously to nuclear translocation, phosphorylation of p65 occurred on Ser536 in both treatments (Fig. 3d), and apart from abrogating further p65 nuclear translocations TVX also lowered its phosphorylation at Ser536 after 120 min to values comparable to levels at 0 min (Fig. 3d).

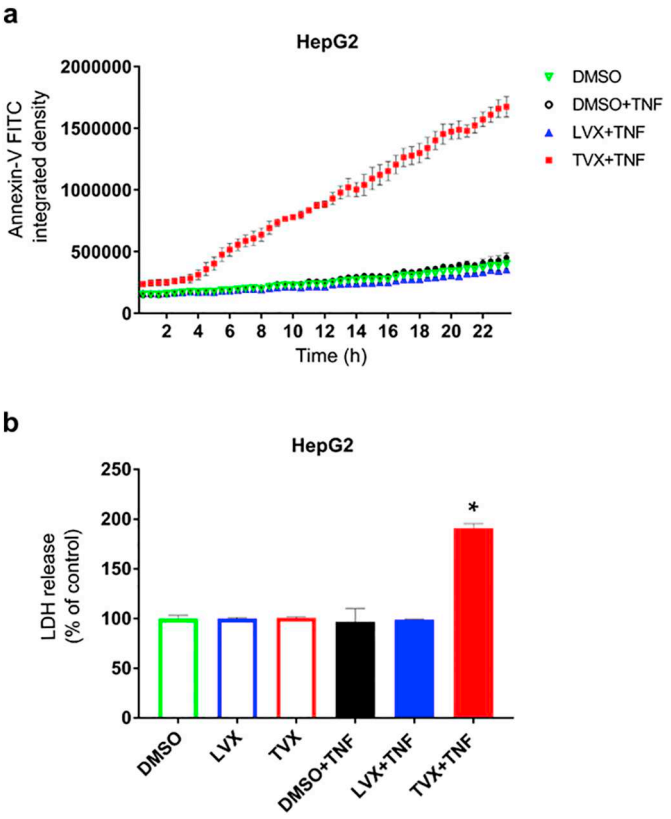

Fig. 2. TVX + TNF induced cell death in HepG2.
HepG2 cells were incubated for 24 h in presence of TVX, LVX or DMSO with or without TNF (4 ng/mL). (a) Treatment with TVX + TNF induces apoptosis in HepG2 cells (increased annexin V-Alexa633 fluorescence). Presented data are representative results for the experiments which were performed three times (b) Coherently, only TVX + TNF significantly increased the LDH in the supernatant of HepG2 cells, here shown for analyzes 24 h after incubation. Data are presented as mean ± SEM; * $p < .05$ when compared with all the other treatments assessed.

3.3. TVX affects TNF-induced expression of NF-κB-related genes

The translocation of NF-κB is a finely orchestrated process, defining transcription of downstream target genes which can be categorized as early (e.g. encoding cytokines and negative regulators of NF-κB pathway), mid (e.g. anti-apoptotic genes) and late (e.g. cell surface receptors) factors (Tian et al., 2005; Zambrano et al., 2016). To obtain further mechanistic insights into the effects of TVX, we set out to examine the kinetics of transcription and translation of NF-κB-related genes (early, middle and late) in presence of TVX + TNF, LVX + TNF and DMSO + TNF.

3.4. TVX increases expression of early NF-κB-related factors A20 and IκBα

Both A20 (TNFAIP3) and IkBα are early NF-κB target genes (Tian et al., 2005). The combination of TVX + TNF caused a higher increase in the transcription of A20 and IκBα in liver homogenates (Fig. 4a) as well as HepG2 cells (Fig. 4c) 2 h after TNF injection or incubation when

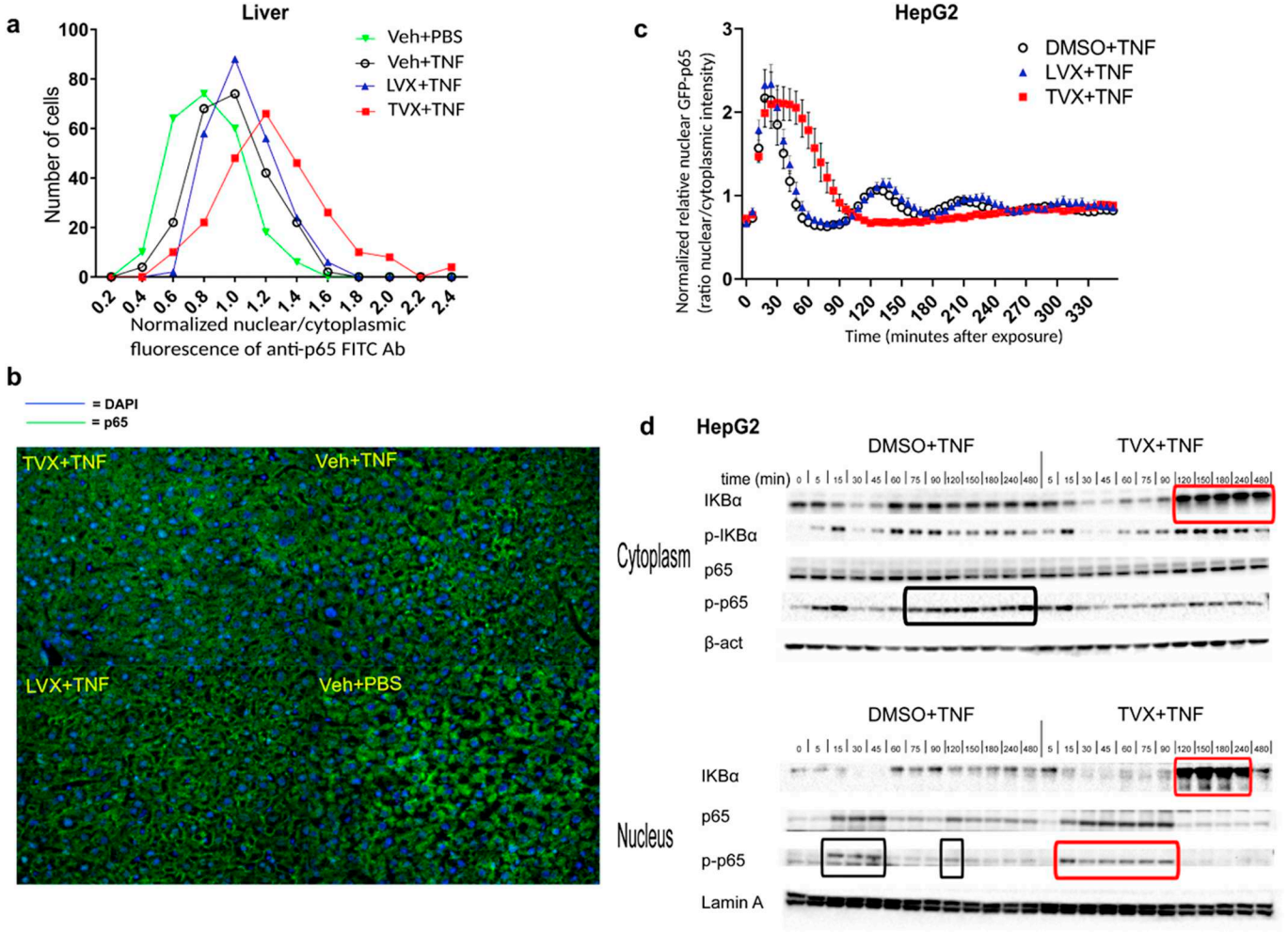

Fig. 3. TVX + TNF disrupted TNF-induced p65 activation and translocation.
Mice were administered with the drug solutions (TVX 150 mg/kg, LVX 375 mg/kg) or the Veh and 3 h after they were intraperitoneally injected with TNF. Livers were excised 2 h after the injection and prepared for immunofluorescent staining of p65. p65-GFP HepG2 and HepG2 cells were incubated with the drug solutions (TVX 20 μM, LVX 50 μM) in presence of TNF (4 ng/mL). At the time point indicated HepG2 cells were lysed and nuclear/cytoplasmic cellular fractionation was performed as mentioned in material and methods. (a-b) TVX + TNF increased the number of hepatocytes with higher nuclear/cytoplasmic ratio. (c) Determination of p65-GFP nuclear-cytoplasmic ratio of genetically modified HepG2 revealed that TVX interferes with p65 oscillation. (d) Fractionation of HepG2 showed that IκBα was accumulated in both cellular fractions at 120 min after exposure to TVX + TNF combination. Phosphorylated p65 at Ser536 was detectable in the nuclear extract of HepG2 cells treated with DMSO + TNF between 15 and 45 min, whereas TVX prolonged its nuclear permanence up to 90 min. Representative blots of 3 experiments are presented. Presented data on GFP-p65 and FITC-anti-p65 fluorescence are results of experiments which were performed three times.

compared with respective controls (Veh + TNF in vivo and DMSO + TNF in vitro). By contrast, the hepatic protein levels of IκBα were decreased upon TVX + TNF treatment 2 h after TNF when compared to all other groups receiving the cytokine (LVX + TNF, Veh + TNF) (Fig. 4b). In HepG2, − LVX + TNF also elicited a significant increase, in A20 mRNA after 1 h of incubation when compared with cells treated with DMSO + TNF (Fig. 4d). Whereas the LVX + TNF-induced increase of A20 mRNA was not reflected by protein expression of the GFP-A20 in HepG2 cells (Fig. 4e), TVX + TNF induced delayed and sustained A20 expression which was associated with higher expression of GFP-A20 beginning 2 h after incubation (Fig. 4e).

Nuclear and cytoplasmic extracts from TVX + TNF-incubated cells showed an accumulation of IκBα in both cellular fractions. Remarkably, higher and stable levels of IκBα were observed from 2 to 4 h in the nuclear extracts and up to 8 h in the cytoplasmic fractions obtained from TVX + TNF-treated HepG2 (Fig. 3c).

3.5. TVX induces different transcriptional regulation of NF-κB-induced inhibitors of apoptosis

TNF-mediated activation of NF-κB causes expression of anti-apoptotic genes, including the IAP family members. Veh + TNF- or LVX + TNF-treatment of mice resulted in increased expression of c-IAP1 in liver homogenates when compared with mice receiving Veh + PBS (Fig. 5a). By contrast, in TVX + TNF-treated mice c-IAP1 mRNA expression was equal to the expression observed in mice receiving Veh + PBS (Fig. 5a). In HepG2 cells, TVX + TNF significantly decreased c-IAP1 gene expression as observed 4 h after the treatment when compared with their respective controls (Fig. 5b). TVX + TNF also decreased XIAP gene expression which was significantly different from controls at 6 h (Fig. 5c). Conversely, c-IAP2 mRNA showed a significant increase in TVX + TNF-treated cells, apparent at 2 h in association with enhanced peak translocation of NF-κB but followed by a rapid decline at 4 h (Fig. 5d). No differences in XIAP and c-IAP2 mRNA expression were observed either in liver and spleen of mice treated with TVX and TNF (data not shown).

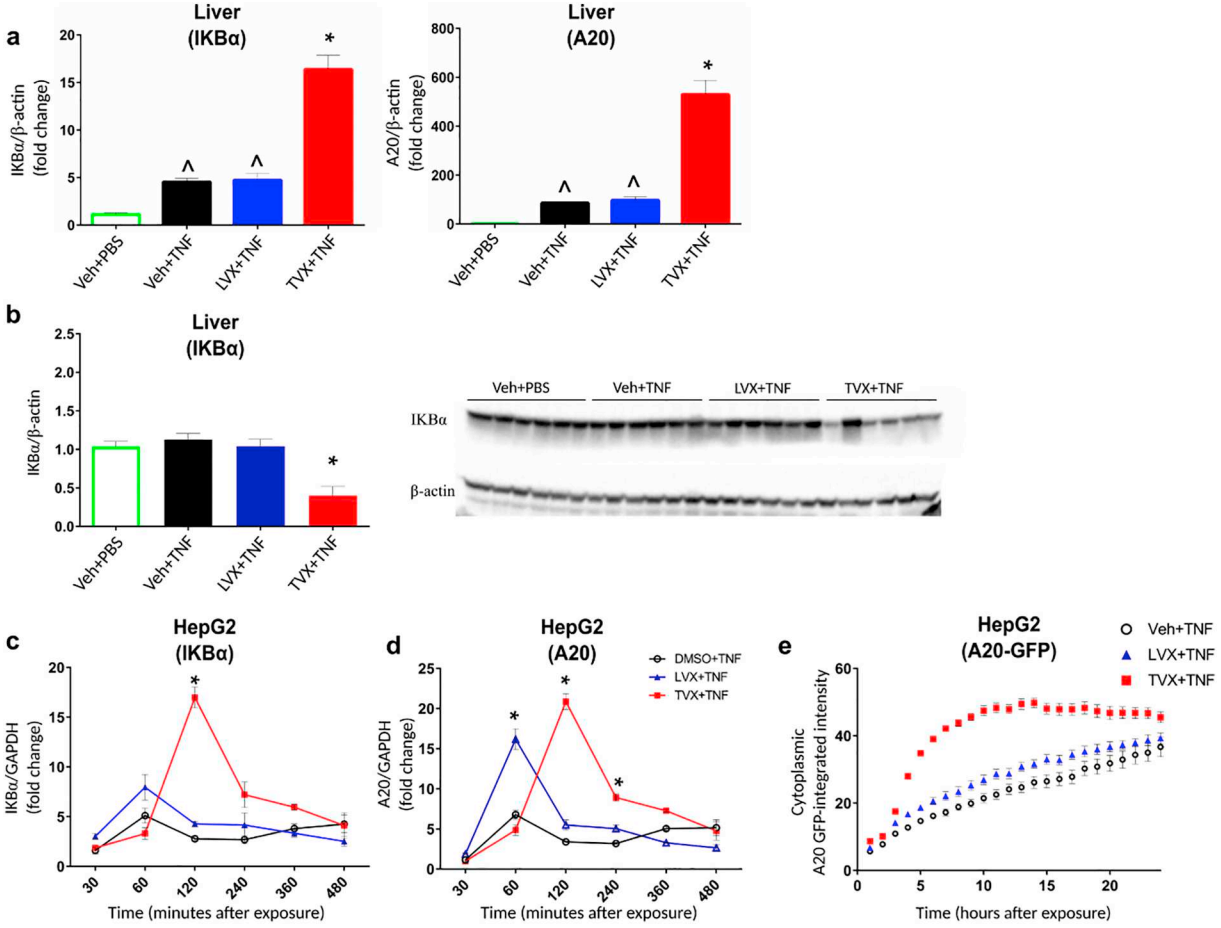

Fig. 4. TVX + TNF increased NF-κB-mediated transcription in vivo and in vitro.
Mice were administered with the drug solutions (TVX 150 mg/kg, LVX 375 mg/kg) or the Veh and 3 h after they were intraperitoneally injected with TNF. Livers were excised 2 h after the injection and the medial part of the biggest lobe was resected and prepared for qPCR or Western blot as reported in material and methods. HepG2 cells were exposed to the drug solutions (TVX 20 μM, LVX 50 μM) containing TNF (4 ng/mL) and prepared for qPCR as reported in materials and methods. (a) TVX + TNF significantly increased the TNF-induced mRNA transcription of IκBα (left panel) and A20 (right panel) in liver when compared with LVX + TNF- or Veh + TNF-treated mice. (b) TVX + TNF significantly decreased hepatic IκBα protein levels when compared with the other treatments. (c-d) TVX + TNF significantly increased TNF-induced IκBα (left panel) and A20 (right panel) transcription in HepG2 cells apparent at 2 h after incubation. LVX + TNF significantly increased the TNF-induced transcription of A20 1 h after the exposure when compared with mice receiving Veh + TNF. (e) TVX + TNF, but not LVX + TNF, significantly enhanced the fluorescence by GFP-A20 HepG2 cells. Fold increase was calculated by comparison with liver or cell lysates were exposed to Veh + PBS or DMSO + PBS. Presented data for GFP-A20 expression are representative results of experiments which were performed three times. All the other data are presented as mean ± SEM; * $p < .05$ when compared with all the other treatments assessed at the same time point; ^ $p < .05$ when compared with liver homogenates obtained from mice receiving only the Veh without TNF.

3.6. TVX reduces ICAM-1 expression

ICAM-1 is a late NF-κB target gene involved in pro-inflammatory responses (Tian et al., 2005). TVX + TNF increased the number of ICAM-1 mRNA copies when compared with any of the other treatments, with a clear increase at 6 h after treatment (Fig. 5e). By contrast, TVX prevented protein expression of ICAM-1 from 8 h of incubation onward (Fig. 5f, squares). LVX + TNF did not affect the TNF-induced protein expression of GFP-ICAM-1 within the 24 h incubation. Importantly, all mice receiving TNF, independently of the drug administered, increased the expression of ICAM-1 mRNA in liver at 2 h time point (Fig. 5g). At the same time point, the TNF-induced ICAM-1 expression was lower in TVX + TNF-treated mice compared to other TNF-treated groups (Fig. 5g). By contrast, no differences in ICAM-1 transcription was observed in the spleens of different treatment groups (data not shown).

3.7. TVX alone affects transcription of NF-κB related genes

To better understand the effects of TVX on TNF-induced transcription and pathway activation we tested the effect of TVX at the same time points without TNF both in vivo and in vitro. Remarkably, the hepatic transcription of A20 and IκBα was also increased 3 h after the TVX administration (Fig. 6a and b), and analogously, the protein levels of IκBα (Fig. 6c). TVX alone significantly reduced c-IAP1 mRNA expression 3 h after oral administration in liver homogenates when compared with the other assessed treatments (Fig. 6d) but not in spleen (data not shown). A significant decrease of ICAM-1 was observed 3 h after drug administration in the liver of either TVX-treated and LVX-treated mice when compared with the control (Fig. 6e). No differences in XIAP and c-IAP2 mRNA expressions were observed either in liver and spleen 3 h after drug administration (data not shown).

In HepG2, TVX (20 μM) alone already caused a small but clear increase in the transcription of both A20 and IκBα, being significant respectively from 2 and 4 h after incubation onward (Fig. 7a and b). After 2 h of exposure with TVX we also observed by Western blot analysis significant increases in cytoplasmic protein expression of IκBα (Fig. 7c and d) and A20 (Fig. 7e) when compared with DMSO-treated cells. Between 2 and 8 h, protein levels of IκBα and A20 increased in time in TVX-treated cells (Fig. 7c-e). LVX itself did not exert any significant effect on the expression of these factors (Fig. 7a-h). TVX significantly

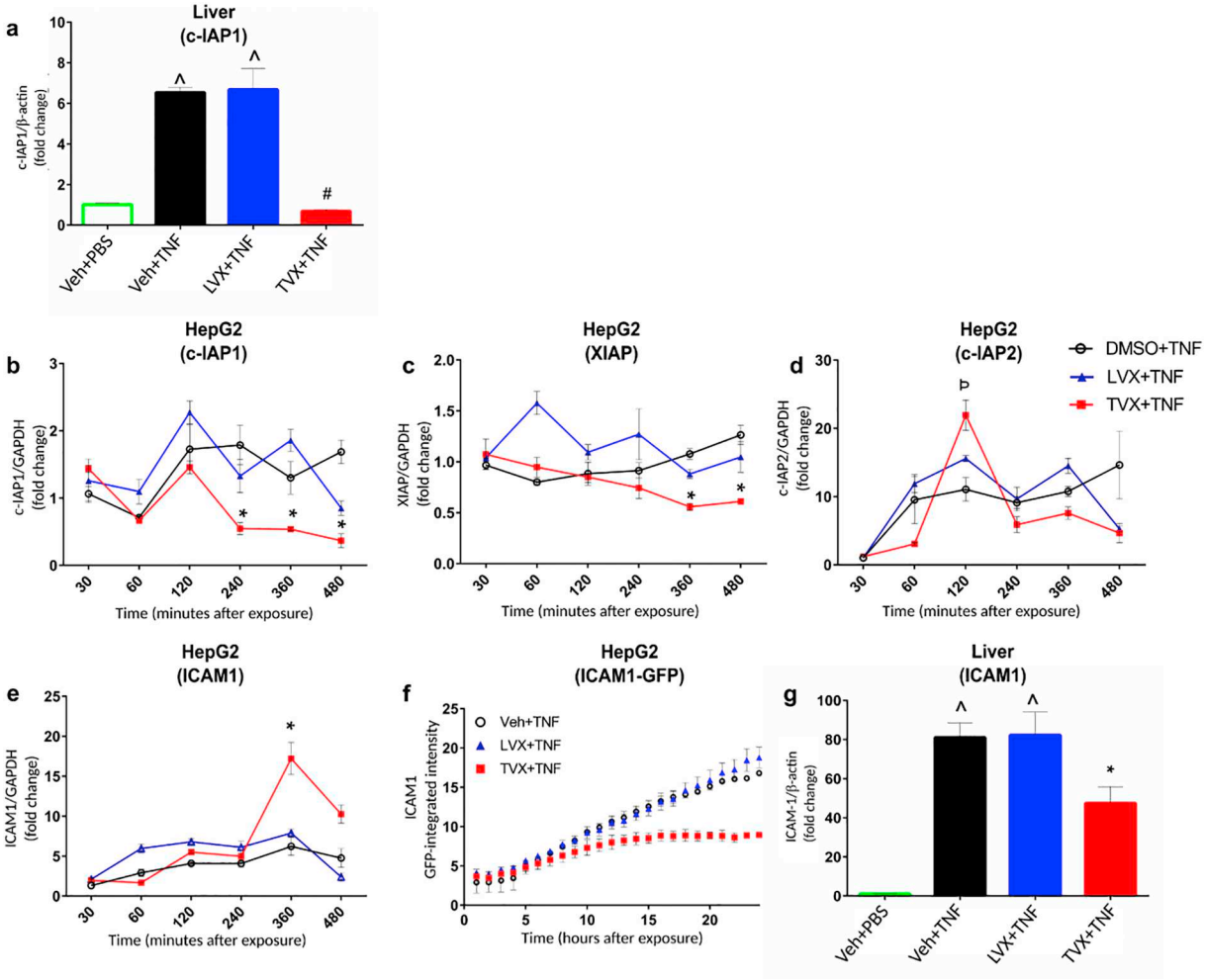

Fig. 5. TVX decreased c-IAP1 and ICAM-1 expression in vivo and in vitro.
Mice were administered with the drug solutions (TVX 150 mg/kg, LVX 375 mg/kg) or the Veh and 3 h after they were intraperitoneally injected with TNF. Livers were excised 2 h after the injection and the medial part of the biggest lobe was resected and prepared for qPCR as reported in material and methods. HepG2 cells were exposed to the drug solutions (TVX 20 μM, LVX 50 μM) containing TNF (4 ng/mL) and prepared for qPCR as reported in materials and methods at the time point indicated in figure. (a) TVX + TNF did not increase the hepatic c-IAP1 mRNA copies as observed in the liver of mice receiving Veh + TNF and LVX + TNF. (b,c) In HepG2, TVX + TNF significantly decreased the mRNA expression of c-IAP1 and XIAP respectively 4 and 6 h after incubation when compared with any other treatment. (d) TVX + TNF significantly increased the expression of c-IAP2 mRNA in HepG2 cells 2 h after incubation when compared with cells exposed to DMSO + TNF. (e) TVX + TNF significantly increased ICAM-1 mRNA 6 h after incubation with HepG2 cells when compared with any other treatment. Fold increase was calculated by comparison with liver or cell lysates that respectively were exposed to Veh + PBS and DMSO + PBS. GFP-ICAM-1 modified HepG2 cell were exposed for 24 h to the indicated treatments (TVX 20 μM, LVX 50 μM) and fluorescence acquired with a confocal laser microscope. (f) TVX + TNF was associated with a significant reduction of GFP-ICAM-1 fluorescence intensity at 8 h when compared with any other assessed treatment. (g) TVX + TNF significantly decreased hepatic ICAM-1 mRNA copies when compared with mice receiving Veh + TNF or LVX + TNF. Data are presented as mean ± SEM; * $p < .05$ when compared with all the other treatments assessed at the same time point; ^ $p < .05$ when compared with liver homogenates obtained from mice receiving only the Veh without TNF; Þ $p < .05$ when compared with cells incubated with DMSO + TNF.

decreased c-IAP1 gene expression as observed 4 h after the treatment of HepG2 cells when compared with cells receiving DMSO (Fig. 7f). XIAP showed the same tendency to decrease after TVX exposure when compared with cells incubated with DMSO but resulting significantly different at 6 h (Fig. 7g). Incubation of HepG2 cells with TVX, LVX or DMSO did not change either transcription and translation of ICAM-1 gene (data not shown).

TVX exposure in RAW264.7 cells resulted in increased transcription of A20, IκBα but not of TNF (Supplemental data) already 2 h after the incubation with the drugs when compared the same cells incubated with DMSO or LVX.

3.8. TVX itself induced p65 translocation in HepG2

The increased transcription of IκBα and A20 in mice pretreated with TVX before TNF injection prompted us to investigate if TVX by itself already affected p65 translocation. We therefore followed the kinetics of the p65-GFP fluorescence in HepG2 cells for 8 h upon incubation with TVX, LVX or the solvent DMSO in absence of TNF. Data shows that TVX alone induced a profound non-oscillatory p65-GFP translocation into the nucleus beginning immediately after incubation and terminating approximately 120 min after the exposure, whereas LVX or DMSO did not exert any effect on p65 translocation (Fig. 8a).

3.9. TVX increases transcription of NF-κB-dependent genes via prolongation of LPS-induced NF-κB translocation in murine RAW264.7 macrophages

The prolongation of NF-κB translocation observed in presence of TVX prompted us to investigate if this also occurred in macrophages after LPS stimulation. Indeed, LPS stimulation of e.g. toll-like receptors

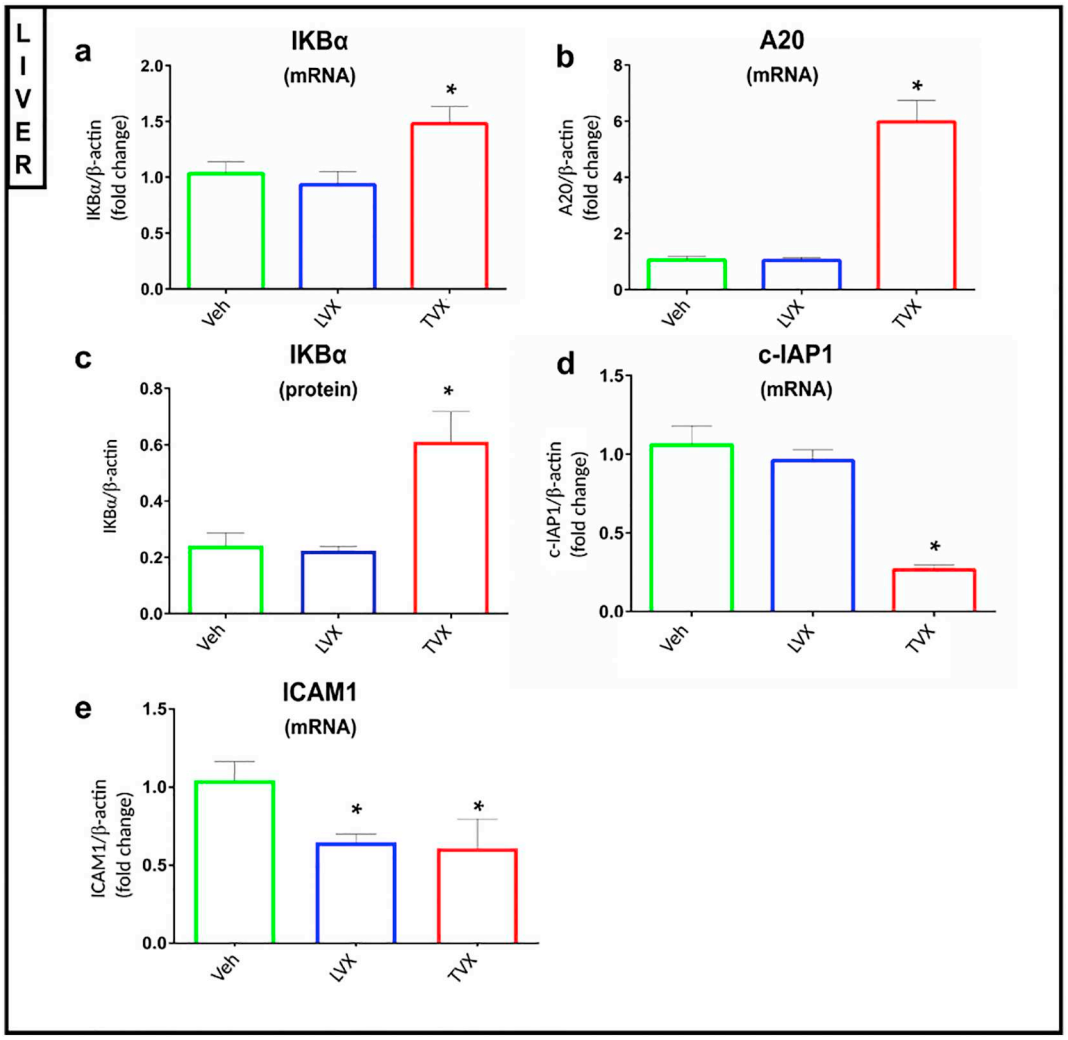

Fig. 6. TVX increased hepatic IκBα and A20 expression and reduced those of ICAM-1 and c-IAP1 in vivo.
Mice were fasted for 7 h and then orally administered with the drug solutions (TVX 150 mg/kg, LVX 375 mg/kg). Three hours after mice were culled, and the medial part of the biggest lobe was resected and prepared for qPCR or western blot as reported in material and methods. (a,b) TVX administration was associated with an increase of IκBα and A20 mRNA and of (c) IκBα protein expression in liver lysates when compared with those of mice treated with LVX or Veh. (d) TVX significantly reduced the mRNA copies of c-IAP1 in liver lysates when compared with the levels observed in those of mice receiving LVX or Veh. (e) TVX and LVX treatments were associated with a reduced ICAM-1 expression in liver lysates when compared with that observed in mice treated with only Veh. Data are presented as mean ± SEM; * $p < .05$ when compared with all the other treatments assessed at the same time point.

(TLRs) induces translocation of NF-κB resulting in increased synthesis of TNF (Sakai et al., 2017). LPS stimulation of RAW264.7 cells resulted in a significant increase in mRNA copies of NF-κB-dependent genes A20, IκBα and TNF, 30 min after the exposure with the bacterial components (Fig. 9a-c). Two hours after incubation, TVX + LPS sustained the increased expression of TNF and enhanced A20 and IκBα mRNA transcripts (Fig. 9a-c).

To determine if TVX also affected LPS activation of NF-κB in macrophages we performed an intracellular staining with an antibody against the p65 subunit and assessed its nuclear translocation in RAW264.7 cells. DMSO + LPS and LVX + LPS exerted a peak of translocation of p65 in between 10 and 45 min when the nuclear/cytoplasmic ratio of the fluorescence returned to a lower level (Fig. 9d). TVX + LPS prolonged the first peak of p65 translocation from 10 to 60 min when returned to levels of the ratio which were comparable with the other groups of treatment (Fig. 9d).

3.10. TVX prolongs TNF-induced activation of MAPKs and IKKα/β activation in HepG2

Based on the observed variations of TNF-induced expression of NF-κB related genes in HepG2, mouse liver and the effects of TVX, we wanted to define the kinetics of downstream regulators of TNF-receptor activation, such as IKKα/β and MAPK (JNK1/2, ERK, p38). Of relevance, JNK activation is critical in the synergistic TNF-induced cytotoxicity caused by other toxicants, including diclofenac (Fredriksson et al., 2011; Maiuri et al., 2015) and cisplatin (Benedetti et al., 2013).

TVX + TNF co-incubation led to a prolonged activation of IKKα/β and the other MAPKs (especially JNK1/2 and ERK) when compared with cells incubated with DMSO + TNF (Fig. 10). Phosphorylation of IKKα/β (Fig. 10a,c) and JNK1/2 (Fig. 10a-b) took place between 15 and 45 min in TNF-treated HepG2 cells, whereas TVX extended their activation up to 90 min (Fig. 10). Cells treated with TVX + TNF showed also a significant increase in ERK and JNK1/2 activation after 8 h when compared with DMSO + TNF-treated cells (Fig. 10a).

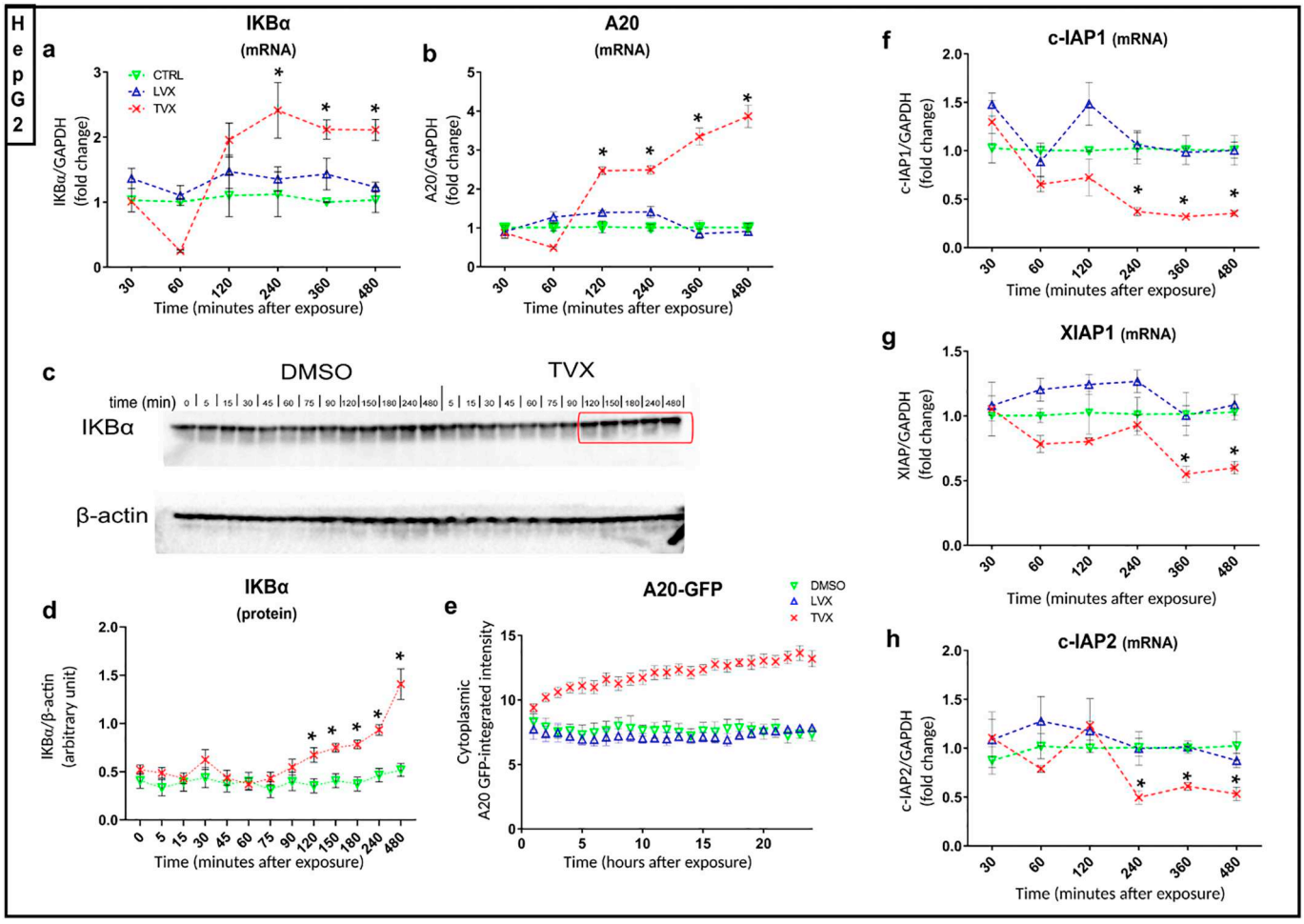

Fig. 7. TVX increased expression of IκBα and A20 in HepG2.
HepG2 cells were incubated with TVX (20 μM), LVX (50 μM) and DMSO for the time showed in figure. At each time point cells were lysed and prepared for qPCR or western blot as mentioned in materials and methods. (a-b) TVX increased the mRNA copies of IκBα and A20 respectively 4 and 2 h after drug incubation when compared with cells exposed to DMSO. (c-d) TVX significantly increased the IκBα protein levels in HepG2 2 h after incubation when compared with cells exposed to DMSO. Representative blot is presented. (f-h) TVX significantly decreased the mRNA expression of c-IAP1, XIAP and c-IAP2 in HepG2 at the incubation time indicated in figure, whereas LVX and DMSO did not exert any significant effect. GFP-A20 modified HepG2 were exposed to the drug solutions and then fluorescence was assessed every hour for 24 h. (e) Increased GFP fluorescence was observed in the cytoplasm of TVX-treated HepG2 during the 24 h of exposure. No significant variance in the cytoplasmic GFP fluorescence was observed in modified HepG2 incubated with LVX or DMSO. Presented data on cytoplasmic A20 expression are representative results for the experiments which were performed three times. Other data are presented as mean ± SEM; * $p < .05$ when compared with all the other treatments assessed at the same time point.

4. Discussion

In order to improve drug safety and prevent new potential hepatotoxic pharmaceuticals reaching the market it is imperative to elucidate possible mechanisms behind the development of DILI. The main challenges are to identify processes that explain (part of) the idiosyncrasy and immune involvement in these adverse reactions.

Although previous experiments on HepG2 and RAW264.7 cells have demonstrated the involvement of DNA Damage Response (DDR) in TVX-induced hepatotoxicity (Poulsen et al., 2014; Beggs et al., 2014) the events leading to the activation of MAPKs and increased synthesis of pro-inflammatory cytokines have not been characterized previously.

In this study, we show that TVX affected several molecular processes by itself, but in particular modulated processes triggered by TNF (in hepatocytes) or by LPS (in macrophages). We demonstrate that unlike the characteristic TNF-induced oscillatory nuclear translocation of NF-κB in HepG2, TVX + TNF combination promoted a single and prolonged translocation of NF-κB into the nucleus. The suppressive effect on p65 translocation was accompanied by enhanced accumulation of known NF-κB inhibitors A20 and IκBα, genes that are activated early after TNF treatment. By contrast, interference with TNF-mediated NF-κB oscillatory translocation by TVX was associated with a decreased transcription of NF-κB-associated middle and late factors (XIAP, c-IAP1 and ICAM-1). The prolongation of TNF-induced NF-κB translocation by TVX appears to be due to extended activation of IKKα/β and related to MAPKs activation. Similarly to what we observed in HepG2, TVX also prolonged LPS-induced p65 translocation in RAW264.7 cells and increased expression of A20, IκBα and TNF. We propose that the enhanced early expression of negative regulators of pro-inflammatory signaling suppresses the later expression of anti-apoptotic and pro-inflammatory molecules. In particular the lack of suppressors of apoptosis, such as IAPs, will allow the onset of apoptosis.

The TVX-induced increased mRNA expression of IκBα was associated with elevated p65 nuclear/cytoplasmic ratio in vivo. The apparent contradiction between in vivo expression of IκBα mRNA and protein prompted us to further characterize the TNF-induced

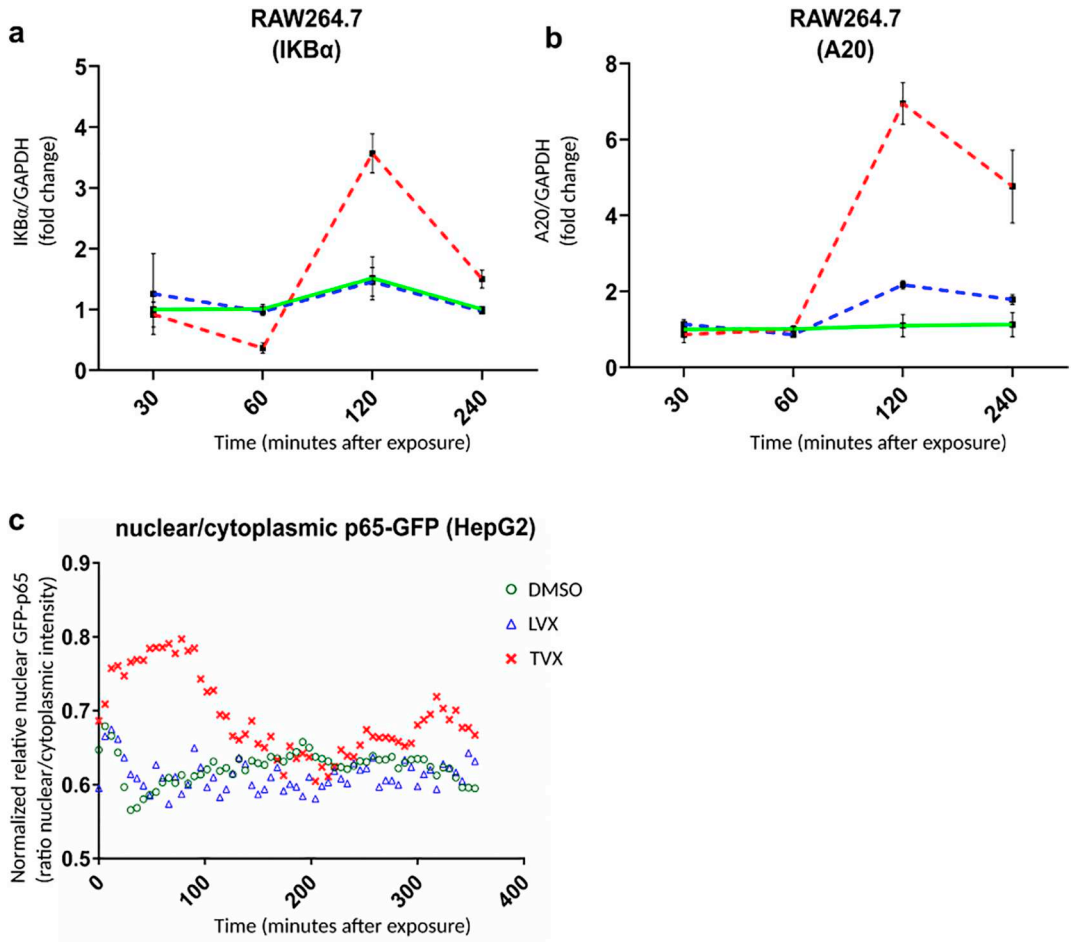

Fig. 8. TVX induced p65 nuclear translocation in HepG2.
Fluorescence of GFP-p65 expressing HepG2 was assessed for 6 h (every 6 min) with a laser confocal microscope as reported in material and methods. RAW264.7 cells were incubated with the drug solution or vehicle for max 4 h. Samples were collected every 30 min and prepared for qPCR as reported in materials and methods. (a) TVX induced an increased GFP-p65 ratio in genetically modified HepG2 beginning immediately after exposure with the drug and terminating approximatively 120 min after. No effects on GFP-p65 localization was observed with LVX or DMSO treatment. (b-c) TVX significantly increased the expression of IκBα and A20 2 h after incubation. Whereas expression of IκBα mRNA in TVX-exposed cells returned to vehicle levels at 4 h, A20 mRNA transcripts were still significantly increased. * $p < .05$ when compared with all the other treatments assessed at the same time point. Presented data for GFP-p65 translocation are representative results for the experiments which were performed three.

translocation of NF-κB in presence of TVX in vitro in HepG2. TVX + TNF doubled the duration of the first nuclear peak of p65 which was phosphorylated at Ser536. Since phosphorylation of p65 determines its transcriptional activity (Sakurai et al., 1999), it was important to note that p65 was phosphorylated at Ser536 residues for the complete duration of the unique translocation occurring in TVX + TNF treated cells. This evidence well explains the increased protein expression of early NF-κB-dependent genes IκBα and A20.

The aberrant expression of NF-κB inhibitors IκBα and A20 occurring after exposure with TVX + TNF may in turn explains the abrogation of secondary NF-κB oscillations. Other studies have demonstrated that NF-κB translocation and transcription is inhibited by expression of a non-degradable IκBα mutant or by overexpression of native IκBα in hepatocytes in vivo and in vitro (Lavon et al., 2000; Xu et al., 1998; Van Antwerp et al., 1996; Park et al., 2001). Moreover, TNF stimulation of hepatocytes expressing non-degradable IκBα resulted in the prevention of NF-κB translocation and the induction of JNK-mediated apoptosis (Liu et al., 2002). In line with these findings, in our experiments with HepG2 cells the inhibition of NF-kB translocations was followed by reactivation of JNK and ERK which both have been demonstrated to play a fundamental role in TVX + TNF-induced cell death (Beggs et al., 2015, 2014). Although we could not demonstrate the direct causality between these events, it is well-known that inhibition of TNF-induced NF-κB translocation induces cell death via JNK pathway and caspase activation (Wullaert et al., 2007; Minero et al., 2013; Liu et al., 2002). Also, the observed downregulation of XIAP and c-IAP1 match with the cytotoxic effects of TVX as both XIAP and c-IAP1 have been demonstrated to inhibit JNK or apoptosis during stimulation with TNF (Wicovsky et al., 2007) but also in the regulation of the NF-κB response during DNA damage (Jin et al., 2009). In addition, previously it has been demonstrated that mono-phasic, non-oscillatory kinetics of NF-κB translocation, as observed with TVX, is particularly accompanied with decreased expression of late genes (e.g. c-IAP1 and ICAM-1) (Tian et al., 2005). Although further investigations are needed, this study provides strong indications that disruption of TNF-induced NF-κB nuclear translocation occurring in presence of TVX + TNF may drive the JNK-dependent apoptosis. All this data, and especially together with the similarities of TVX effects between HepG2 and RAW264.7 on TNF-receptor- or TLR-mediated NF-kB activation stimulated respectively with TNF and LPS, indicates that TVX affects a common downstream molecular target in regulatory pathways of NF-κB and MAPKs. This evidence is, in our opinion, a fundamental finding to orientate future researches

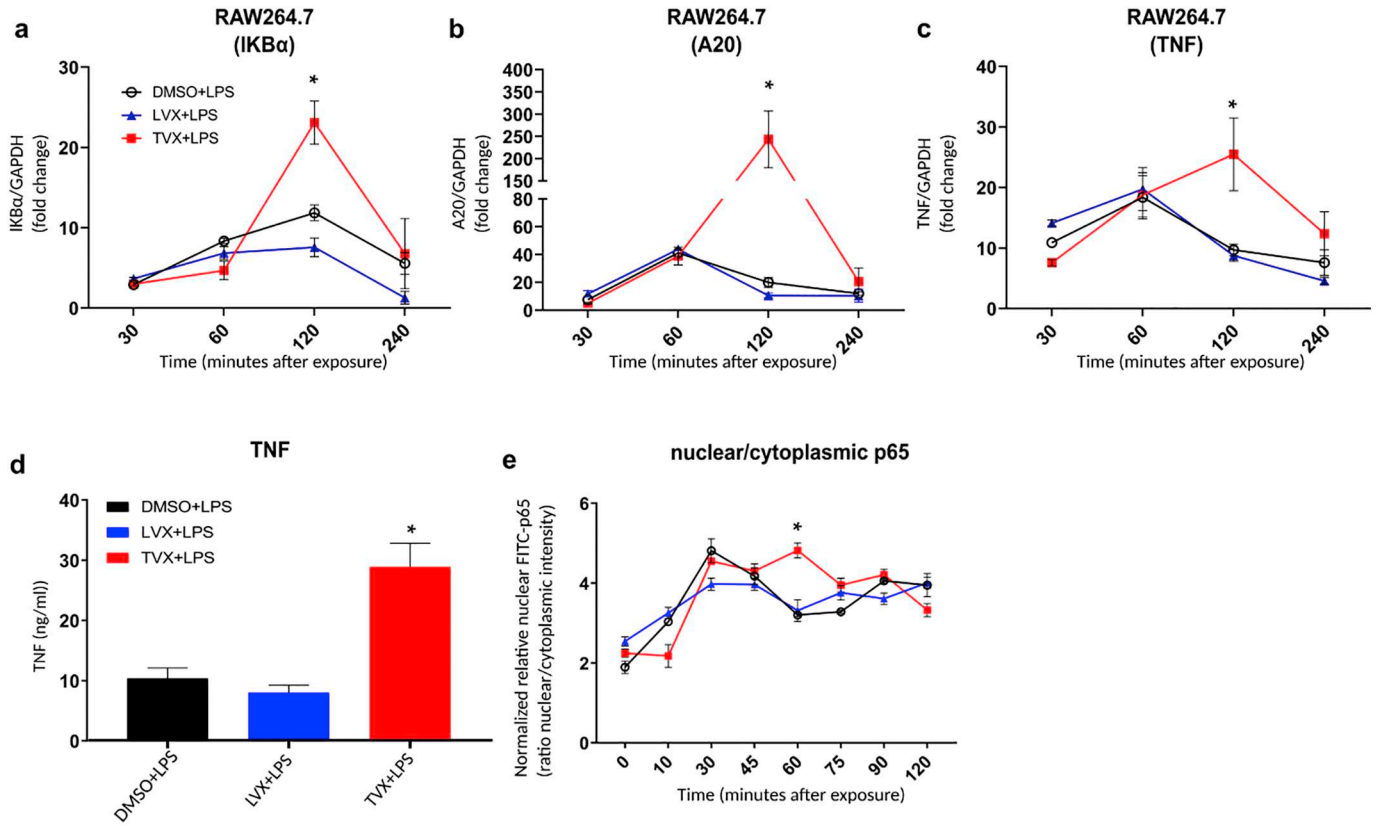

Fig. 9. TVX + LPS increased the expression of IκBα, A20 and TNF in RAW264.7 cells.
RAW264.7 cells were incubated for 2 h with the drug solutions (TVX 20 μM, LVX 50 μM) and then stimulated with LPS (10 ng/mL). At the time point indicated in figure cells were lysed and prepared for qPCR as reported in material and methods. (a,b,c) TVX + LPS significantly increased the mRNA copies of κBα, A20 and TNF when compared with any other assessed treatment 2 h after the addition of the bacterial component. (d) TVX + LPS increased the secretion of TNF in the supernatant of RAW264.7 cells 4 h after the exposure when compared with cell exposed to Veh + LPS or LVX + LPS. For p65 localization RAW264.7 cells were plated in IBIDI μ-slide 8 well and fixed at the time point showed in figure. (e) Detection of FITC-anti-p65 antibody revealed that TVX + LPS prolonged p65 translocation in the nucleus of RAW264.7 up to 75 min whereas DMSO + LPS and LVX + LPS returned to lower ratio values after 60 min. Presented data for FITC-p65 localization are representative results for the experiments which were performed three times. Data are presented as mean ± SEM; * $p < .05$ when compared with all the other treatments assessed at the same time point.

aiming to better characterize the mechanisms behind TVX-induced liver injury and to identify potential hepatotoxic compounds. Moreover, data on RAW cells may add to the understanding of the complexity of the in vivo situation.

In our experiments, we observed that TVX alone, at concentrations which resemble those found in patients' livers (Vincent et al., 1997), already activates transcription of NF-κB associated genes like IκBα and A20. In vitro this was preceded by minor and prolonged translocation of p65 NF-κB subunit into the nucleus of HepG2 cells, within the same time frame in which TNF mediates the transcription factor translocation. These results suggest that TVX itself already initiates NF-κB translocation, which may be linked to the observation of apoptotic cells in livers prior to injection of TNF (Giustarini et al., 2018). This does not exclude the possibility that in vivo hepatotoxic effects of TVX can be reinforced by macrophage activation as result of LPS leaking from the gut (Poulsen et al., 2014).

The presented mechanisms observed for the combined effects of TVX and TNF or LPS exposure provides new insights into the initial steps of TVX-induced liver damage. In addition to the effects observed here, TVX-induced liver damage may also involve lack in regulation of inflammation (Giustarini et al., 2018, 2019), and increased formation of apoptotic bodies due to pannexin-1 inhibition (Poon et al., 2014). The possible interplay of these mechanisms exemplifies the complexity of immune-mediated liver injury caused by a combination of inflammatory stressors and drugs like TVX that can reinforce phlogistic processes.

Obviously the "phenotype" of the adverse reaction in mice, which is an acute form of hepatotoxicity remains distinct from the hypersensitivity and DILI features observed in patients (Ballet, 2015; Kenna and Uetrecht, 2018). Nevertheless, the various key events in TVX-induced adverse reactions, e.g. increased hepatic cell death and macrophage activation, and delayed regulation of inflammation may contribute to sensitization of neoantigen specific T cells as so-called adjuvant processes. Our data also exemplifies that specific activation kinetics of intracellular cascades may represent an adverse outcome pathway for those compounds showing increased hepatotoxicity when combined with TNF. On the other hand, the assessment of these kinetics will allow in vitro identification of aspects of compounds with IDILI liability also when these compounds will not cause direct toxicity on hepatocytes or their most-used models. Downstream effects of dysregulated NF-κB and MAPKs pathways might represent the initiating event for an immune-mediated reaction.

Declaration of Competing Interest

The authors declare that they have no known competing financial interests or personal relationships that could have appeared to influence the work reported in this paper.

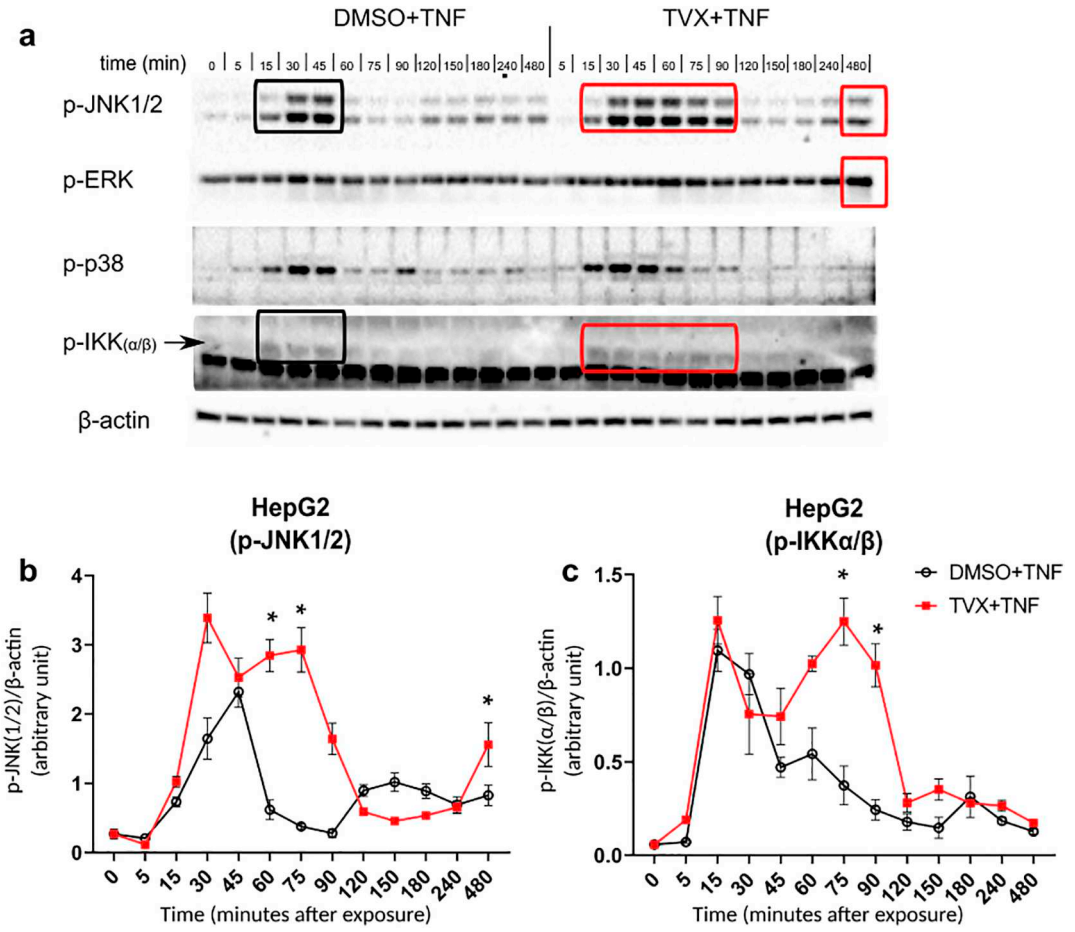

Fig. 10. TVX + TNF showed prolonged IKKα/β and JNK1/2 phosphorylation.
HepG2 cells were incubated with the drug-cytokine combinations, lysed at the time point indicated in figure and processed as reported in material and methods. (a,b) TVX + TNF mainly prolonged JNK1/2 and (a,c) IKKα/β phosphorylation mediated by TNF receptor activation when compared with cells treated with DMSO + TNF. Representative blots of 3 experiments are presented. Data are presented as mean ± SEM; * $p < .05$ when compared with all the other treatments assessed at the same time point.

Acknowledgements

This work was supported by the European Community (Grant number MIP-DILI-115336). The Mechanism-Based Integrated Systems for the Prediction of Drug-Induced Liver Injury (MIP-DILI) project has received support from the Innovative Medicines Initiative Joint Undertaking, resources of which are composed of financial contribution from the European Union's Seventh Framework Programme (FP7/20072013) and EFPIA companies' in-kind contribution. http://www.imi.europa.eu/.

References

Ballet, F., 2015. Preventing drug-induced liver injury: how useful are animal models? Dig. Dis. 33, 477–485.
Beggs, K.M., et al., 2014. Molecular mechanisms of hepatocellular apoptosis induced by Trovafloxacin-tumor necrosis factor-alpha interaction. Toxicol. Sci. 137, 91–101.
Beggs, K.M., et al., 2015. Trovafloxacin-induced replication stress sensitizes HepG2 cells to tumor necrosis factor-alpha-induced cytotoxicity mediated by extracellular signal-regulated kinase and ataxia telangiectasia and Rad3-related. Toxicology 331, 35–46.
Benedetti, G., et al., 2013. TNF-α-mediated NF-κB survival signaling impairment by cis-platin enhances JNK activation allowing synergistic apoptosis of renal proximal tubular cells. Biochem. Pharmacol. 85, 274–286.
Buchweitz, J.P., 2002. Underlying Endotoxemia augments toxic responses to chlorpro-mazine: is there a relationship to drug idiosyncrasy? J. Pharmacol. Exp. Ther. 300, 460–467.
Chalasani, N., et al., 2015. Features and outcomes of 899 patients with drug-induced liver injury: the DILIN prospective study. Gastroenterology 148, 1340–1352 e7.
Copeland, S., et al., 2005. Acute inflammatory response to endotoxin in mice and humans acute inflammatory response to endotoxin in mice and humans. Clin. Diagn. Lab. Immunol. 12, 60–67.
Deng, X., et al., 2006. Modest inflammation enhances diclofenac hepatotoxicity in rats: role of neutrophils and bacterial translocation. J. Pharmacol. Exp. Ther. 319, 1191–1199.
Dugan, C., MacDonald, A., 2010. A mouse model of severe halothane hepatitis based on human risk factors. J. Pharmacol. Exp. Ther. 333, 364–372.
Fontana, R.J., et al., 2009. Drug-induced liver injury network (DILIN) prospective study: rationale, design and conduct. Drug Saf. 32, 55–68.
Fredriksson, L., et al., 2011. Diclofenac inhibits tumor necrosis factor-α-induced nuclear factor-κB activation causing synergistic hepatocyte apoptosis. Hepatology 53, 2027–2041.
Fredriksson, L., et al., 2014. Drug-induced endoplasmic reticulum and oxidative stress responses independently sensitize toward TNFα-mediated hepatotoxicity. Toxicol. Sci. 140, 144–159.
Giustarini, G., et al., 2018. Tissue influx of neutrophils and monocytes is delayed during development of trovafloxacin - induced tumor necrosis factor - dependent liver injury in mice. J. Appl. Toxicol. 38, 753–765.
Giustarini, G., et al., 2019. Trovafloxacin-induced liver injury: lack in regulation of in-flammation by inhibition of nucleotide release and neutrophil movement. Toxicol. Sci. 167, 385–396.
Herpers, B., et al., 2016. Activation of the Nrf2 response by intrinsic hepatotoxic drugs correlates with suppression of NF-κB activation and sensitizes toward TNFα-induced cytotoxicity. Arch. Toxicol. 90, 1163–1179.
Jin, H.-S., et al., 2009. cIAP1, cIAP2, and XIAP act cooperatively via nonredundant pathways to regulate genotoxic stress-induced nuclear factor-kappaB activation. Cancer Res. 69, 1782–1791.
Kamentsky, L., et al., 2011. Improved structure, function and compatibility for cellpro-filer: modular high-through- put image analysis software. Bioinformatics 27, 1179–1180.
Kenna, J.G., Uetrecht, J., 2018. Do In Vitro assays predict drug candidate idiosyncratic drug-induced liver injury risk? Drug Metab. Dispos. 46, 1658–1669.
Lavon, I., et al., 2000. High susceptibility to bacterial infection, but no liver dysfunction, in mice compromised for hepatocyte NF-κB activation. Nat. Med. 6, 573–577.
Liguori, M.J., et al., 2008. Trovafloxacin-induced gene expression changes in liver-

derived in vitro systems : comparison of primary human hepatocytes to HepG2 cells. Drug Metab. Dispos. 36, 223–233.
Liu, H., et al., 2002. NF-κB inhibition sensitizes hepatocytes to TNF-induced apoptosis through a sustained activation of JNK and c-Jun. Hepatology 35, 772–778.
Lu, J., et al., 2012. Amiodarone exposure during modest inflammation induces idiosyncrasy-like liver injury in rats: role of tumor necrosis factor-alpha. Toxicol. Sci. 125, 126–133.
Luyendyk, J.P., 2003. Ranitidine treatment during a modest inflammatory response precipitates idiosyncrasy-like liver injury in rats. J. Pharmacol. Exp. Ther. 307, 9–16.
Maiuri, A.R., et al., 2015. Cytotoxic synergy between cytokines and NSAIDs associated with idiosyncratic hepatotoxicity is driven by mitogen-activated protein kinases. Toxicol. Sci. 146, 265–280.
Matzinger, P., Kamala, T., 2011. Tissue-based class control: the other side of tolerance. Nat. Rev. Immunol. 11, 221–230.
Minero, V.G., et al., 2013. JNK activation is required for TNFα-induced apoptosis in human hepatocarcinoma cells. Int. Immunopharmacol. 17, 92–98.
Park, G.Y., et al., 2001. Anti-inflammatory effect of adenovirus-mediated IkappaBalpha overexpression in respiratory epithelial cells. Eur. Respir. J. Off. J. Eur. Soc. Clin. Respir. Physiol. 18, 801–809.
Pirmohamed, M., et al., 2002. The danger hypothesis–potential role in idiosyncratic drug reactions. Toxicology 181–182, 55–63.
Poon, I.K.H., et al., 2014. Unexpected link between an antibiotic, pannexin channels and apoptosis. Nature 507, 329–334.
Poulsen, K.L., et al., 2014. Trovafloxacin enhances lipopolysaccharide-stimulated production of tumor necrosis factor-α by macrophages: role of the DNA damage response. J. Pharmacol. Exp. Ther. 350, 164–170.
Puigvert, J.C., et al., 2010. High-throughput live cell imaging of apoptosis. Curr. Protoc. Cell Biol. 1–13.
Roth, R.A., et al., 2017. Idiosyncratic drug-induced liver injury: is drug-cytokine interaction the linchpin? J. Pharmacol. Exp. Ther. 360, 461–470.
Sakai, J., et al., 2017. Lipopolysaccharide-induced NF-κB nuclear translocation is primarily dependent on MyD88, but TNFα expression requires TRIF and MyD88. Sci. Rep. 7, 1–9.
Sakurai, H., et al., 1999. IkB kinases phosphorylate NF-kB p65 subunit on serine 536 in the transactivation domain. J. Biol. Chem. 274, 30353–30356.
Shaw, P.J., et al., 2009a. Trovafloxacin enhances the inflammatory response to a gram-negative or a gram-positive bacterial stimulus, resulting in neutrophil-dependent liver injury in mice. J. Pharmacol. Exp. Ther. 330, 72–78.
Shaw, P.J., et al., 2009b. Tumor necrosis factor α is a proximal mediator of synergistic hepatotoxicity from Trovafloxacin / lipopolysaccharide Coexposure. J. Pharmacol. Exp. Ther. 328, 62–68.
Taudorf, S., et al., 2007. Human models of low-grade inflammation: bolus versus continuous infusion of endotoxin. Clin. Vaccine Immunol. 14, 250–255.
Tian, B., et al., 2005. A TNF-induced gene expression program under oscillatory NF-kappaB control. BMC Genomics 6, 137.
Van Antwerp, D.J., et al., 1996. Suppression of TNF-alpha-induced apoptosis by NF-kappaB. Science 274, 787–789.
Van de Water, B., et al., 2001. Suppression of chemically induced apoptosis but not necrosis of renal proximal tubular epithelial (LLC-PK1) cells by focal adhesion kinase (FAK). Role of FAK in maintaining focal adhesion organization after acute renal cell injury. J. Biol. Chem. 276, 36183–36193.
Vincent, J., et al., 1997. Pharmacokinetics and safety of trovafloxacin in healthy male volunteers following administration of single intravenous doses of the prodrug, alatrofloxacin. J. Antimicrob. Chemother. 39 (Suppl B), 75–80.
Weaver, R.J., et al., 2017. Test systems in drug discovery for hazard identification and risk assessment of human drug-induced liver injury. Expert Opin. Drug Metab. Toxicol. 13, 767–782.
Wicovsky, A., et al., 2007. Sustained JNK activation in response to tumor necrosis factor is mediated by caspases in a cell type-specific manner. J. Biol. Chem. 282, 2174–2183.
Wink, S., et al., 2017. High-content imaging-based BAC-GFP toxicity pathway reporters to assess chemical adversity liabilities. Arch. Toxicol. 91, 1367–1383.
Wink, S., et al., 2018. Dynamic imaging of adaptive stress response pathway activation for prediction of drug induced liver injury. Arch. Toxicol. 92, 1797–1814.
Wullaert, A., et al., 2006. Mechanisms of crosstalk between TNF-induced NF-kappaB and JNK activation in hepatocytes. Biochem. Pharmacol. 72, 1090–1101.
Wullaert, A., et al., 2007. Hepatic tumor necrosis factor signaling and nuclear factor-κB: effects on liver homeostasis and beyond. Endocr. Rev. 28, 365–386.
Xu, Y., et al., 1998. NF-kappaB inactivation converts a hepatocyte cell line TNF-alpha response from proliferation to apoptosis. Am. J. Phys. 275, C1058–C1066.
Yan, K., Verbeek, F.J., 2012. Segmentation for high-throughput image analysis: watershed masked clustering. In: Margaria, T, Steffen, B (Eds.), Lecture notes in computer science (including subseries lecture notes in artificial intelligence and lecture notes in bioin- formatics). Springer, Berlin, pp. 25–41.
Zambrano, S., et al., 2016. NF-κB oscillations translate into functionally related patterns of gene expression. Elife 5, 1–38.
Zou, W., et al., 2009. Hepatotoxic interaction of sulindac with lipopolysaccharide: role of the hemostatic system. Toxicol. Sci. 108, 184–193.